Supporting Information

N-Type Organic Field-Effect Transistors with Very High Electron Mobility Based on Thiazole Oligomers with Trifluoromethylphenyl Groups **

Shinji Ando,[1] Ryo Murakami, [1] Jun-ichi Nishida,[1] Hirokazu Tada,[2]
Youji Inoue,[3] Shizuo Tokito,[3] Yoshiro Yamashita[1]*

[1]Department of Electronic Chemistry, Interdisciplinary Graduate School of Science and Engineering, Tokyo Institute of Technology, Nagatsuta, Midori-ku, Yokohama 226-8502. [2]Institute for Molecular Science, Myodaiji, Okazaki 444-8585.[3] NHK Science and Technical Research Laboratories, Kinuta, Setagaya-ku, Tokyo 157-8510.

E-mail: yoshiro@echem.titech.ac.jp

General. Melting points were obtained on a YANACO melting point apparatus and uncorrected. EI mass spectra were collected on a SHIMADZU GCMS-QP5000 mass spectrometer. UV-vis spectra were recorded on a SHIMADZU MultiSpec-1500. Emission spectra were collected on a SHIMADZU RF-1500 spectrometer. Differential pulse voltammogram and cyclic voltammogram were recorded on a BAS-100B system containing terabutylammonium hexafluorophosphate ($TBAPF_6$) (0.1 mol dm^{-3} in dry dichloromethane or DMF). The Pt disk, Pt wire and SCE were used as the working, counter, and reference electrodes, respectively. Elemental analyses were performed at the Tokyo Institute of Technology, Chemical Resources Laboratory.

Materials. 4-Trifluromethylphenylboronic acid was purchased from Aldrich and used without further purification. Tris(2,4-pentanedionate)iron(Ⅲ) was purchased from Tokyo Kasei Co. and used without further purification. Tetrakis(triphenylphosphine)palladium(0), NaOH, *n*-Butyllithium in *n*-hexane, THF and toluene were purchased from Kanto Chemicals, and used without further purification.

2,2'-Bis(4-trifluoromethylphenyl)-5,5'-bithiazole (1) To a solution of 5-bromo-2-(4-trifluoromethylphenyl)thiazole (380 mg, 1.23 mmol) in THF (50 ml) was added dropwise *n*-BuLi { 0.85 ml (1.35 mmol) of 1.54 M solution in *n*-hexane } within 10 min at –78 ºC. After stirring for 1 h at –78 ºC, a solution of tris(2,4-pentanedionato)Iron(Ⅲ) (433 mg, 1.23 mmol) in THF (20 ml) was added. After warming to room temperature, the mixture was stirring for 3 h and then the solvent was evaporated. The black residue was purified by silica gel column chromatography with dichloromethane and sublimation to give **1** (82 mg, 30%) as yellow crystals. mp 232 - 235 ºC. IR (KBr) ; ν max 629, 847, 976, 1015, 1063, 1105, 1137, 1168, 1319, 1421, 1486, 1614 cm^{-1}. ^{1}H-NMR (300 MHz, $CDCl_3$) δ 7.74 (d, 4H, J = 8.4 Hz), 8.02 (s, 2H), 8.08 (d, 4H, J = 8.1 Hz) ppm. MS (EI) *m/z* 456 (M^+). Anal. Calcd for $C_{20}H_{10}F_6N_2S_2$: C, 52.63; H, 2.21; N, 6.22; S, 13.55. Found: C, 52.71; H, 2.17; N, 6.22; S, 13.55.

2,2'-Bis(4-trifluoromethylphenyl)-2,2'-bithiazole (2) A solution of 5,5'-dibromo-2,2'-bithiazolyl (172 mg, 0.53 mmol), 4-trifluromethylphenylboronic acid (200 mg, 1.1 mmol), tetrakis(triphenylphosphine)palladium(0) (32 mg, 0.027 mmol) and 2 M NaOH (2 mL) in toluene (100 mL) was refluxed for 24 h. The mixture was cooled to room temperature and the solvent was evaporated. The dark green residue was purified by silica gel column chromatography with dichloromethane and sublimation to give **2** (33 mg, 14%) as yellow crystals : mp 227 - 230 ºC. IR (KBr) ; ν max 594, 835, 918, 1016, 1068, 1113, 1173, 1322, 1412, 1614 cm^{-1}. ^{1}H-NMR (300 MHz, $CDCl_3$) δ 7.71 (d, 4H, J = 8.7 Hz), 7.75 (d, 4H, J

= 8.7 Hz) 8.14 (s, 2H) ppm. MS (EI) *m/z* 456 (M^+). Anal. Calcd for $C_{20}H_{10}F_6N_2S_2$: C, 52.63; H, 2.21; N, 6.22; S, 13.55. Found: C, 52.98; H, 2.47; N, 6.12; S, 13.95.

2,2'''-Bis(4-trifluoromethylphenyl)[5,5';2',2'';5'',5''']quaterthiazole (3): A solution of 5-bromo-2-(5-bromothiazol-2-yl)thiazole (409 mg, 1.25 mmol), 5-(tributylstannyl)-2-(4-trifluoromethylphenyl)thiazole (1.30 g, 2.51 mmol) and tetrakis(triphenylphosphine)palladium(0) (72 mg, 0.063 mmol) in toluene (100 mL) was refluxed for 96 h. The mixture was cooled to room temperature and the solvent was evaporated. The dark residue was purified by sublimation to give **3** (70 mg, 12%) as red crystals : mp 350 - 352 ºC. IR (KBr) ; ν max 482, 628, 842, 927, 976, 1014, 1068, 1134, 1324, 1390, 1487, 1615 cm^{-1}. MS (EI) *m/z* 622 (M^+). Anal. Calcd for $C_{26}H_{12}F_6N_4S_4$: C, 50.15; H, 1.94; N, 9.00; S, 20.60. Found: C, 50.33; H, 2.08; N, 9.11; S, 20.81.

2,2'''-Bis(4-trifluoromethylphenyl-2-thiazolyl)-2,2'-bithiophene (4): A solution of 2-bromo-5-(5-bromothiophen-2-yl)thiophene (412 mg, 1.28 mmol), 5-(tributylstannyl)-2-(4-trifluoromethylphenyl)thiazole (1.33 g, 2.56 mmol) and tetrakis(triphenylphosphine)palladium(0) (74 mg, 0.064 mmol) in toluene (100 mL) was refluxed for 96 h. The mixture was cooled to room temperature and the solvent was evaporated. The dark residue was purified by sublimation to give **4** (148 mg, 18%) as red crystals : mp 307 - 309 ºC. IR (KBr) ; ν max 479, 629, 794, 849, 972, 1069, 1110, 1135, 1325, 1429, 1486, 1614 cm^{-1}. MS (EI) *m/z* 620 (M^+). Anal. Calcd for $C_{28}H_{14}F_6N_2S_4$: C, 54.18; H, 2.27; N, 4.51; S, 20.66. Found: C, 54.46; H, 2.54; N, 4.37; S, 20.53.

2,2'''-Bis(4-trifluoromethylphenyl-2-thenyl)-2,2'-bithiazole (5): A solution of 5-bromo-2-(5-bromothiazol-2-yl)thiazole (472 mg, 1.45 mmol), 5-(tributylstannyl)-2-(4-trifluoromethylphenyl)thiazole (1.50 g, 2.89 mmol) and tetrakis(triphenylphosphine)palladium(0) (83 mg, 0.072 mmol) in toluene (100 mL) was refluxed for 96 h. The mixture was cooled to room temperature and the solvent was evaporated. The dark residue was purified by sublimation to give **5** (51 mg, 6%) as red crystals : mp 285 - 287 ºC. IR (KBr) ; ν max 802, 839, 927, 1062, 1077, 1113, 1174, 1324, 1390, 1613 cm^{-1}. MS (EI) *m/z* 620 (M^+). Anal. Calcd for $C_{28}H_{14}F_6N_2S_4$: C, 54.18; H, 2.27; N, 4.51; S, 20.66. Found: C, 54.55; H, 2.26; N, 4.70; S, 21.05.

5,5'''-Bis(4-trifluoromethylphenyl)[2,2';5',2'';5'',2''']quaterthiophene (6): A solution of 2-bromo-5-(5-bromothiophen-2-yl)thiophene (150 mg, 0.47 mmol), 5-(tributylstannyl)-2-(4-trifluoromethylphenyl)thiazole (482 mg, 0.93 mmol) and

tetrakis(triphenylphosphine)palladium(0) (27 mg, 0.023 mmol) in toluene (100 mL) was refluxed for 96 h. The mixture was cooled to room temperature and the solvent was evaporated. The dark residue was purified by sublimation to give **6** (25 mg, 9%) as red crystals : mp 332 - 333 °C. IR (KBr) ; ν max 599, 699, 792, 839, 1015, 1068, 1080, 1131, 1175, 1326, 1411, 1441, 1613 cm^{-1}. MS (EI) *m/z* 618 (M^+). Anal. Calcd for $C_{30}H_{16}F_6S_4$: C, 58.24; H, 2.61; S, 20.73. Found: C, 58.24; H, 2.81; S, 22.29.

X-ray analysis. The measurements of thiazole derivatives **1–2** were carried out on a Rigaku RAXIS-RAPID Imaging Plate diffractometer (Mo-Kα radiation, λ = 0.71075 Å). The data were collected at 93 K and the structure was solved by the direct method (SIR97) and refined by the full matrix least-squares method on F^2 with the anisotropic temperature factors for non-hydrogen atoms. Hydrogen atoms of **1–2** were placed in geometrically calculated positions. Absorption correction was applied using empirical procedure. **1**: crystal size: 0.80 × 0.60 × 0.20 mm. monoclinic, *C2/m*, *Z* = 2. *a* = 18.58(2), *b* = 6.736(5), *c* = 7.380(7) Å, β = 104.70(4)° *V* = 893(5) $Å^3$, $2\theta_{max}$ = 55.0°, ρ_{calcd} = 1.697 g/cm^3. Of 4233 reflections, 1102 were unique (R_{int} = 0.033), 88 parameters, R_1 = 0.039, wR_2 = 0.112 (for all reflections). **2**: crystal size: 0.70 × 0.20 × 0.10 mm. triclinic, P-1, *Z* = 2. *a* = 4.688(6), *b* = 13.37(2), *c* = 14.57(2) Å, α =99.62(6), β = 97.97(5) γ =94.74(6)° , *V* = 886(7) $Å^3$, $2\theta_{max}$ = 55.0°, ρ_{calcd} = 1.756 g/cm^3. Of 8314 reflections, 3950 were unique (R_{int} = 0.032), 271 parameters, R_1 = 0.054, wR_2 = 0.076 (for all reflections).

Fabrication of OFETs. OFETs were constructed on heavily doped n-type silicon wafers covered with 2000 Å-thick thermally grown silicon dioxide. The silicon dioxide acts as a gate dielectric layer, and the silicon wafer serves as a gate electrode. Organic compounds were deposited on the silicon dioxide by vacuum evaporation at a rate of 0.3–0.5 $Å s^{-1}$ under pressure of 10^{-4} Pa. The thickness of the semiconductor layer was 500 Å. During the evaporation, the temperature of the substrate was maintained by heating a copper block on which the substrate was mounted. Gold was used as source and drain electrodes and deposited on the organic semiconductor layer through a shadow mask with a channel width (*W*) of 1000 μm and a channel length (*L*) of 100, 75, 50 μm. Finally, the FET measurements were carried out at room temperature in the vacuum chamber (10^{-5} Pa) without exposure to air with Hewlett-Packard 4140A and 4140B models.

X-ray Diffraction Studies. X-ray diffraction (XRD) measurements were carried out with a JEOL JDX-3530 X-ray diffractometer system. XRD patterns were obtained using Bragg-Brentano geometry with CuKα radiation as an X-ray source with an acceleration voltage of 40 kV and a beam current of 30 mA.

AFM Studies. AFM measurements were made in air using a Digital Instruments Nanoscope III in tapping mode.

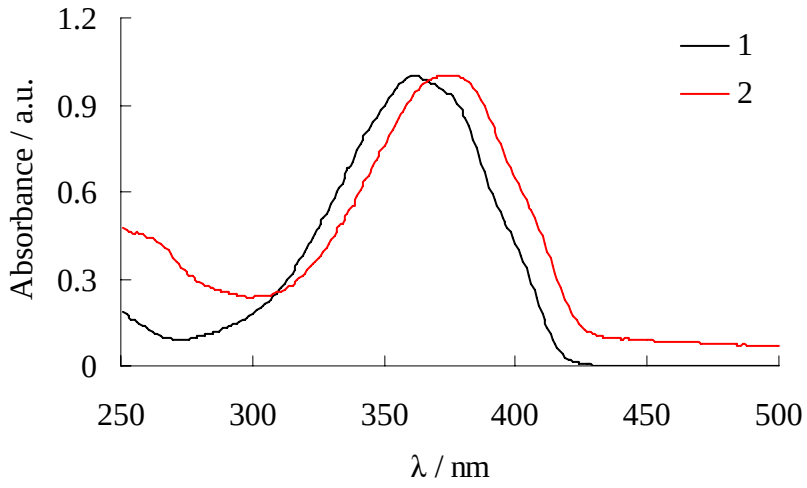

Figure S1. Absorption spectra of **1**–**2** in $CHCl_3$.

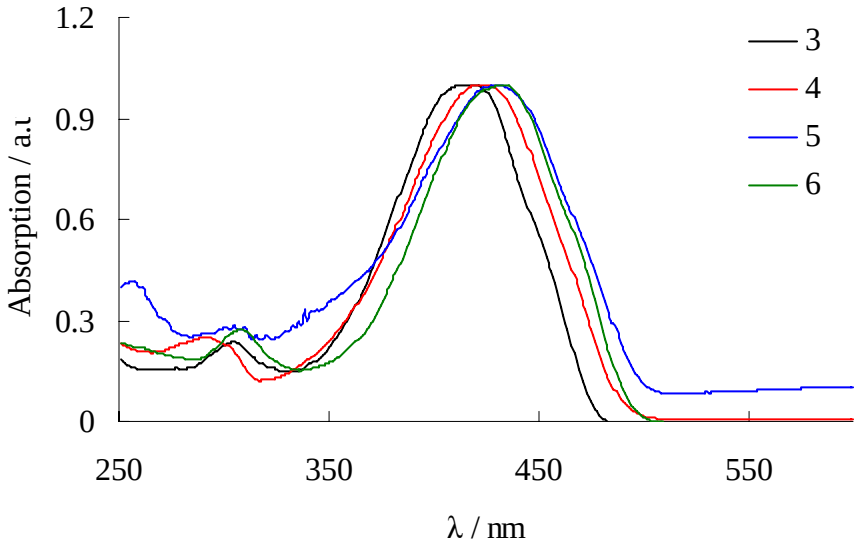

Figure S2. Absorption spectra of **3**–**6** in $CHCl_3$.

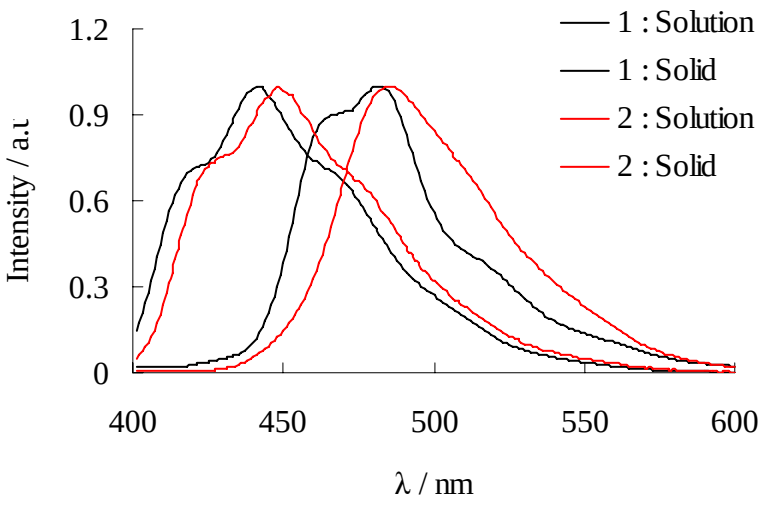

Figure S3. Emission spectra of **1**–**2** in $CHCl_3$ and solid.

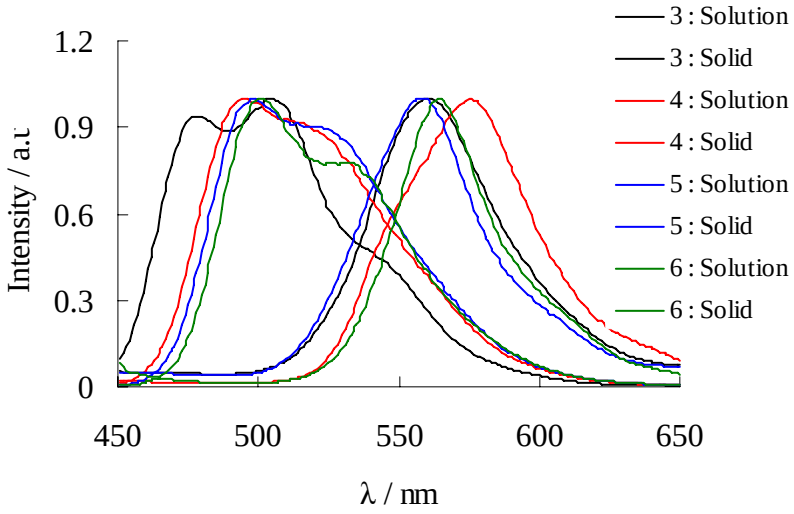

Figure S4. Emission spectra of **3**–**6** in $CHCl_3$ and solid.

Table S1. Absorption and fluorescene maxima of oligomers **1**–**6** in the chloroform and solid state.

Compound	Solution		Solid
	λ_{abs} (nm)	λ_{em} (nm)	λ_{em} (nm)
1	**363**	**442**	**481**
2	**372**	**448**	**486**
3	**417**	**504**	**559**
4	**442**	**495**	**576**
5	**430**	**498**	**559**
6	**432**	**502**	**564**

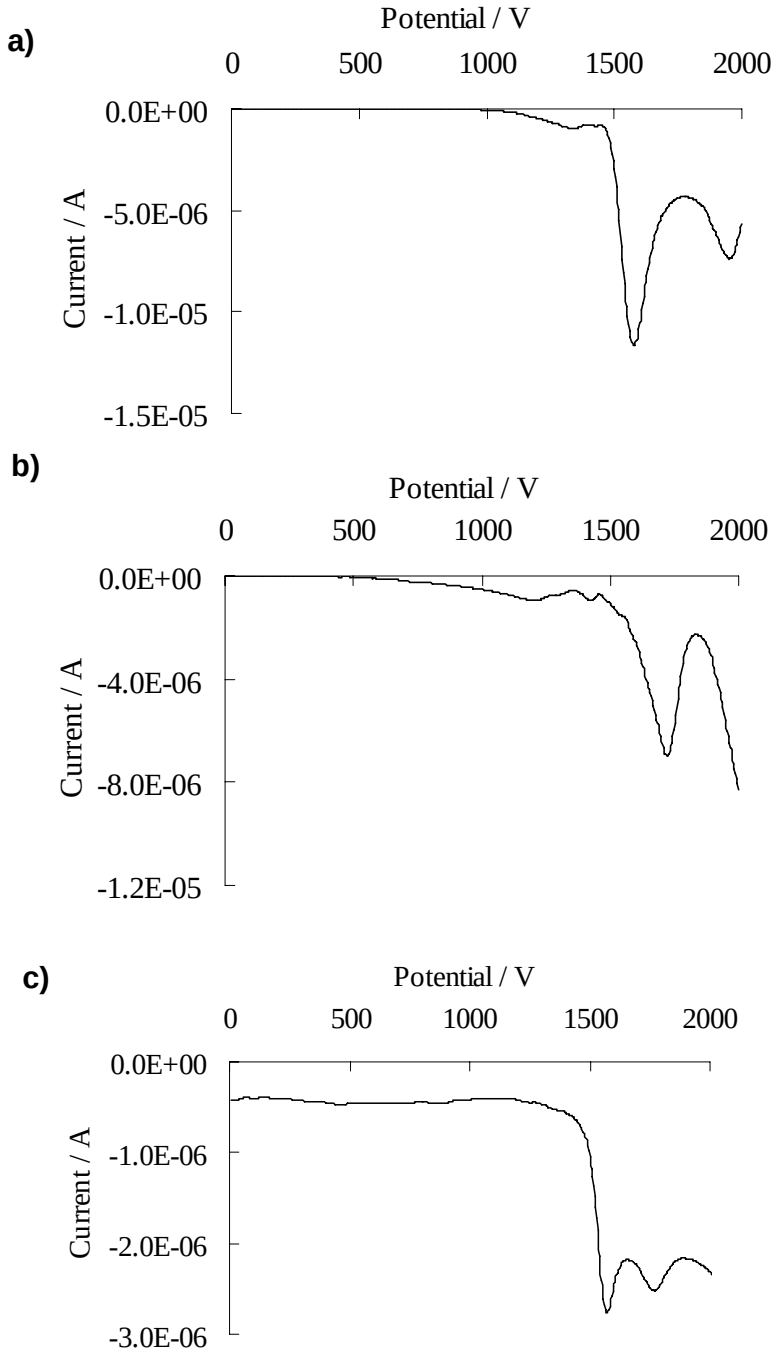

Figure S5. Differential pulse voltammograms of oligomers **1** (a), **2** (b) and **3**(c). Conditions: 0.1 M (n-Bu)$_4$NPF$_6$ in dichloromethane.

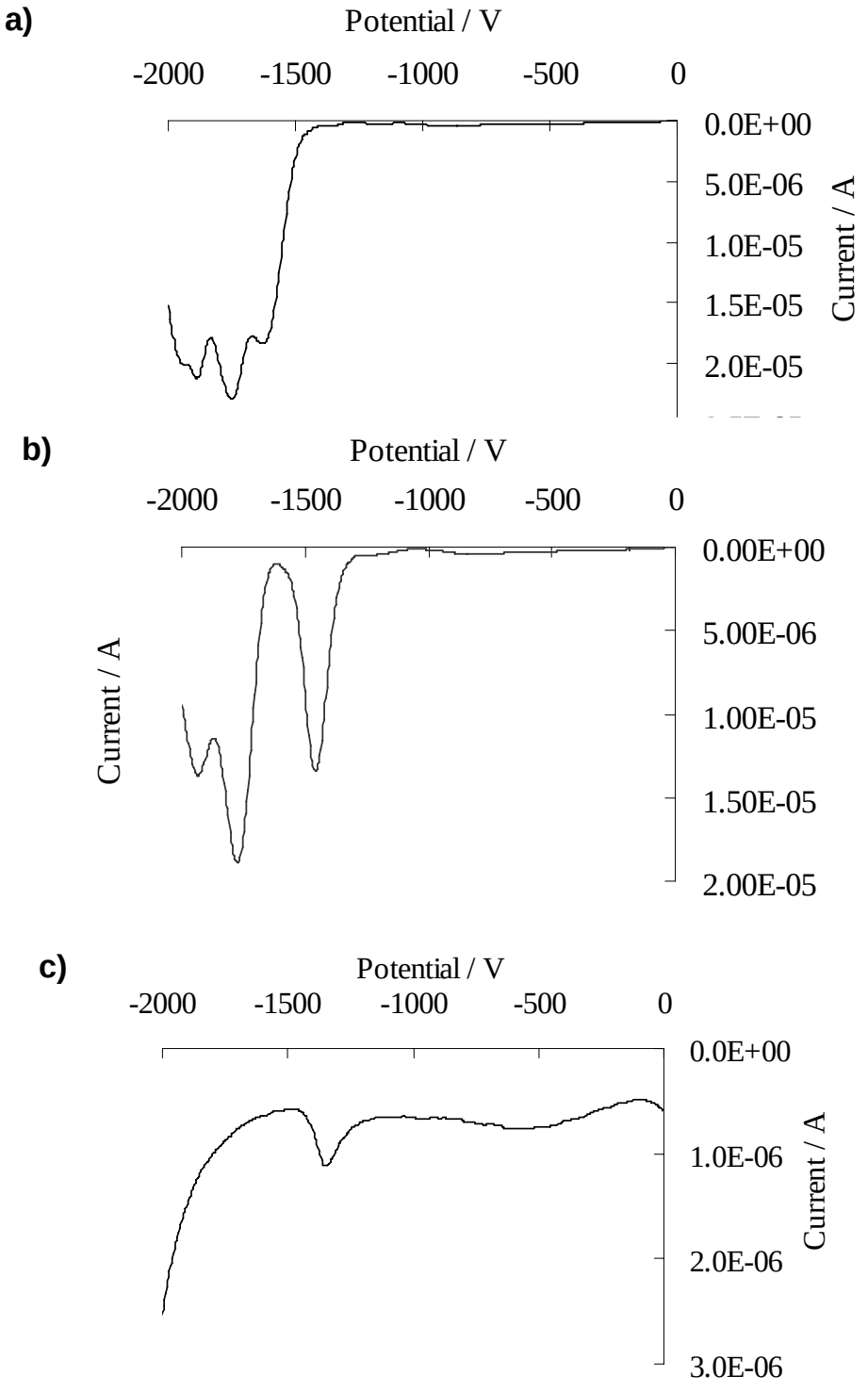

Figure S6. Differential pulse voltammograms of oligomers **1** (a), **2** (b) and **3** (c). Conditions: 0.1 M (n-Bu)$_4$NPF$_6$ in dichloromethane.

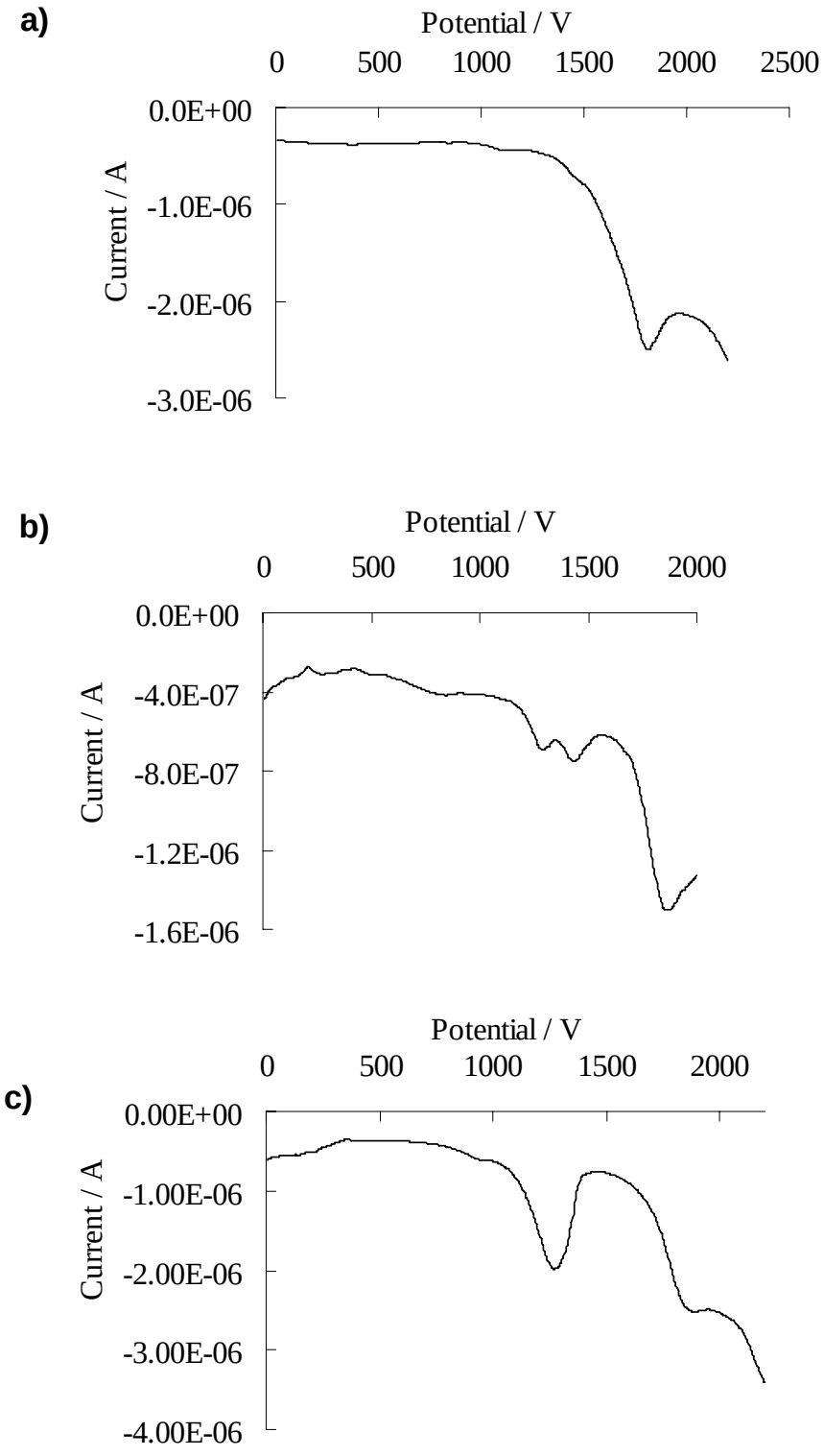

Figure S7. Differential pulse voltammograms of oligomers **4** (a), **5** (b) and **6** (c). Conditions: 0.1 M $(n\text{-Bu})_4NPF_6$ in dichloromethane.

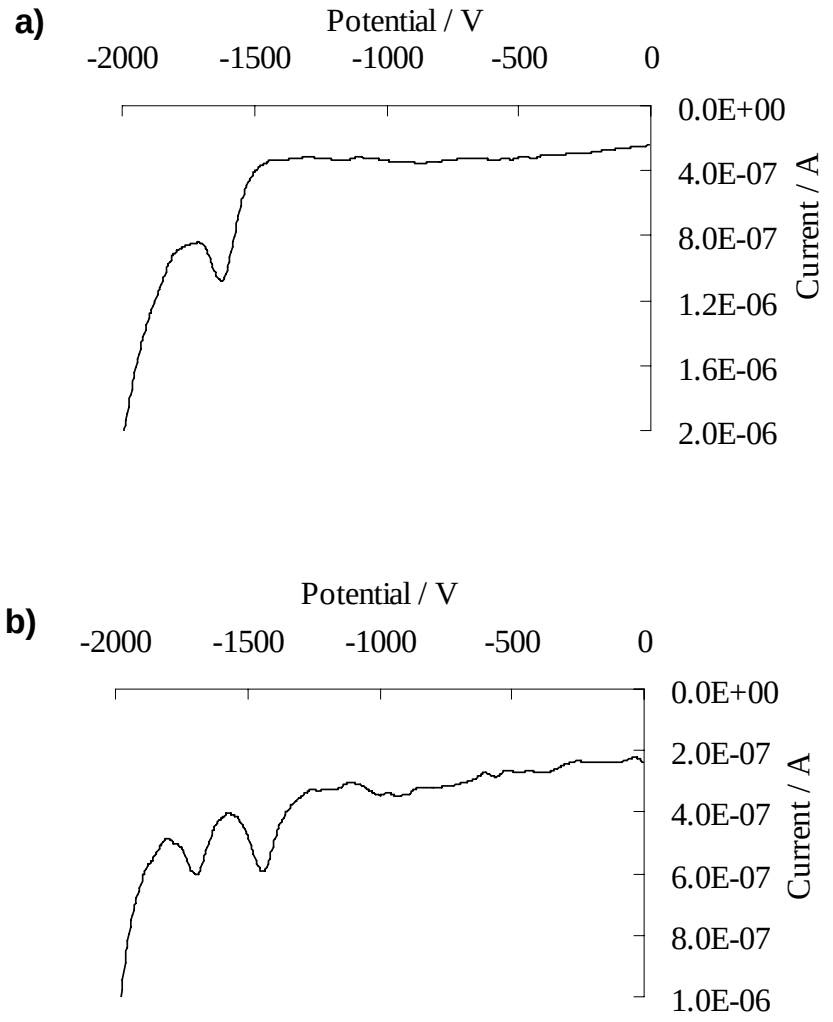

Figure S8. Differential pulse voltammograms of oligomers **4** (a) and **5** (b). Conditions: 0.1 M (n-Bu)$_4$NPF$_6$ in dichloromethane.

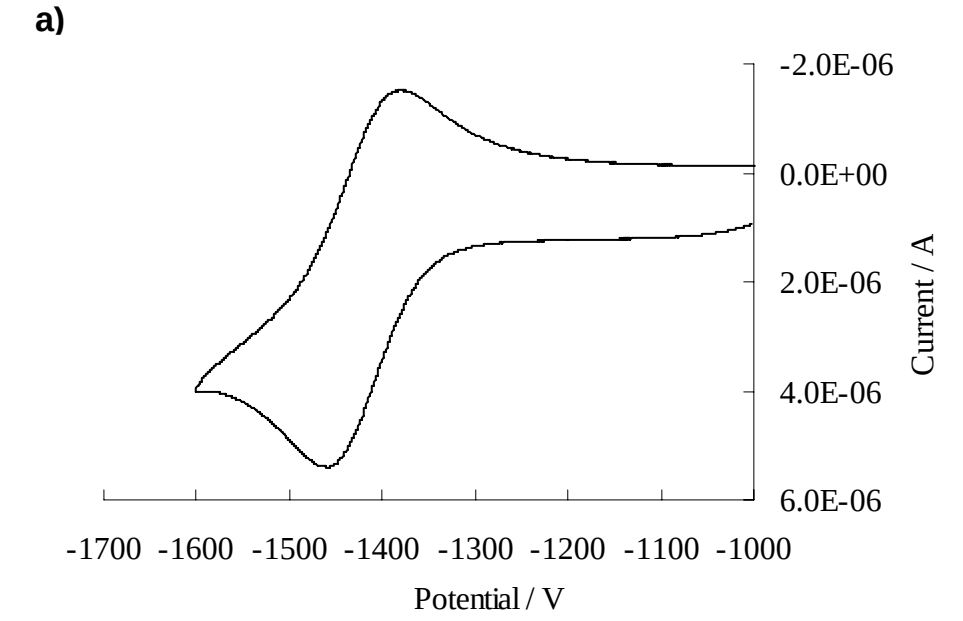

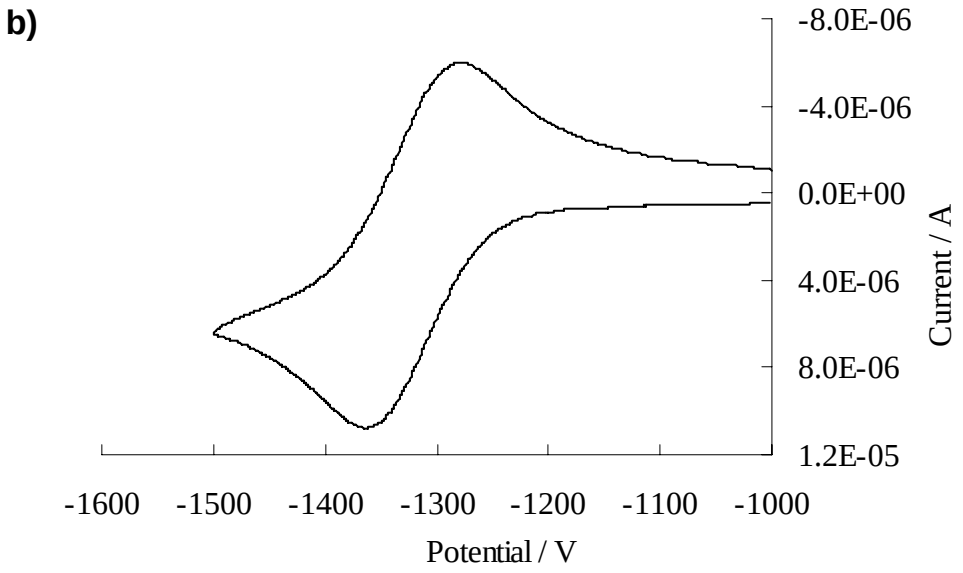

Figure S9. Cyclic voltammograms of oligomer **1** (a) and **2** (b). Conditions: 0.1 M (*n*-Bu)$_4$NPF$_6$ in DMF.

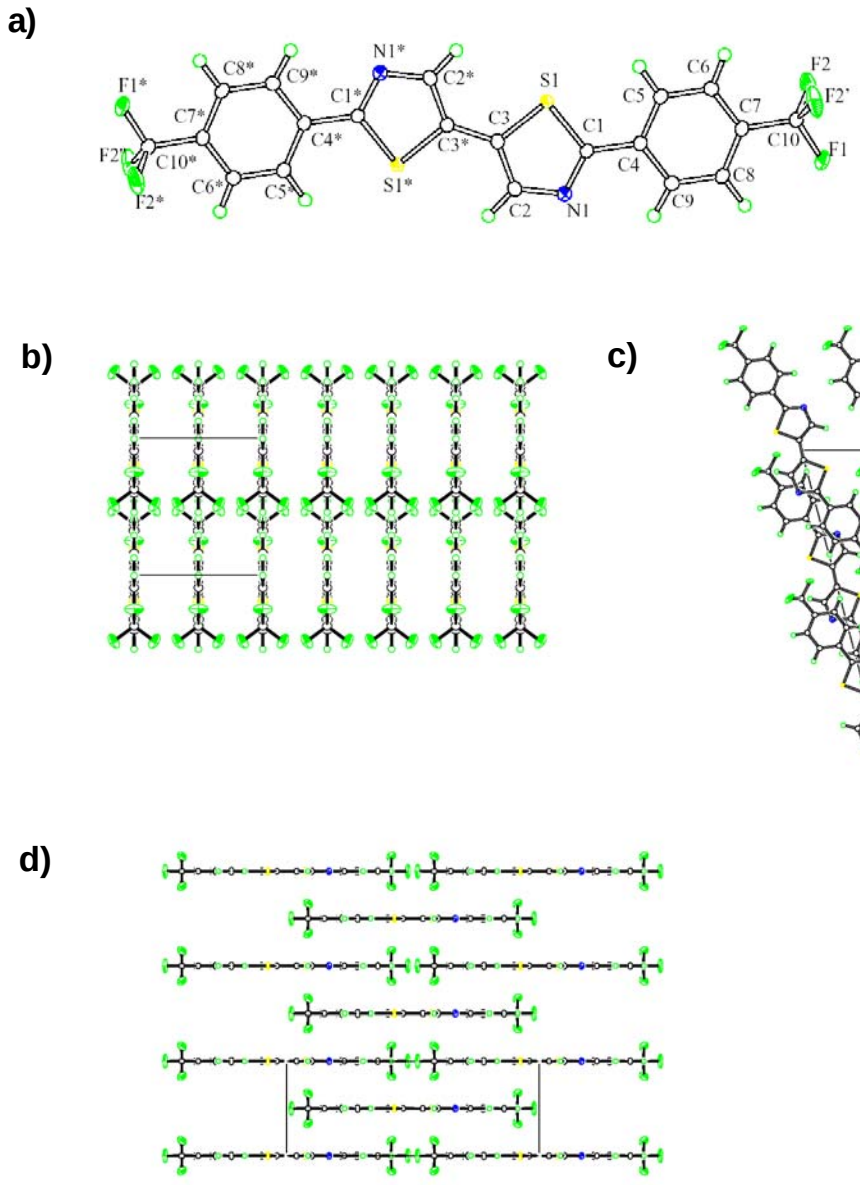

Figure S10. X-ray structure of compound **1**; (a) Molecular structure of **1**. Stacking structure of **1** along the a-axis (b) and the c-axis (d). (c) π– π overlap of **1** along with b-axis.

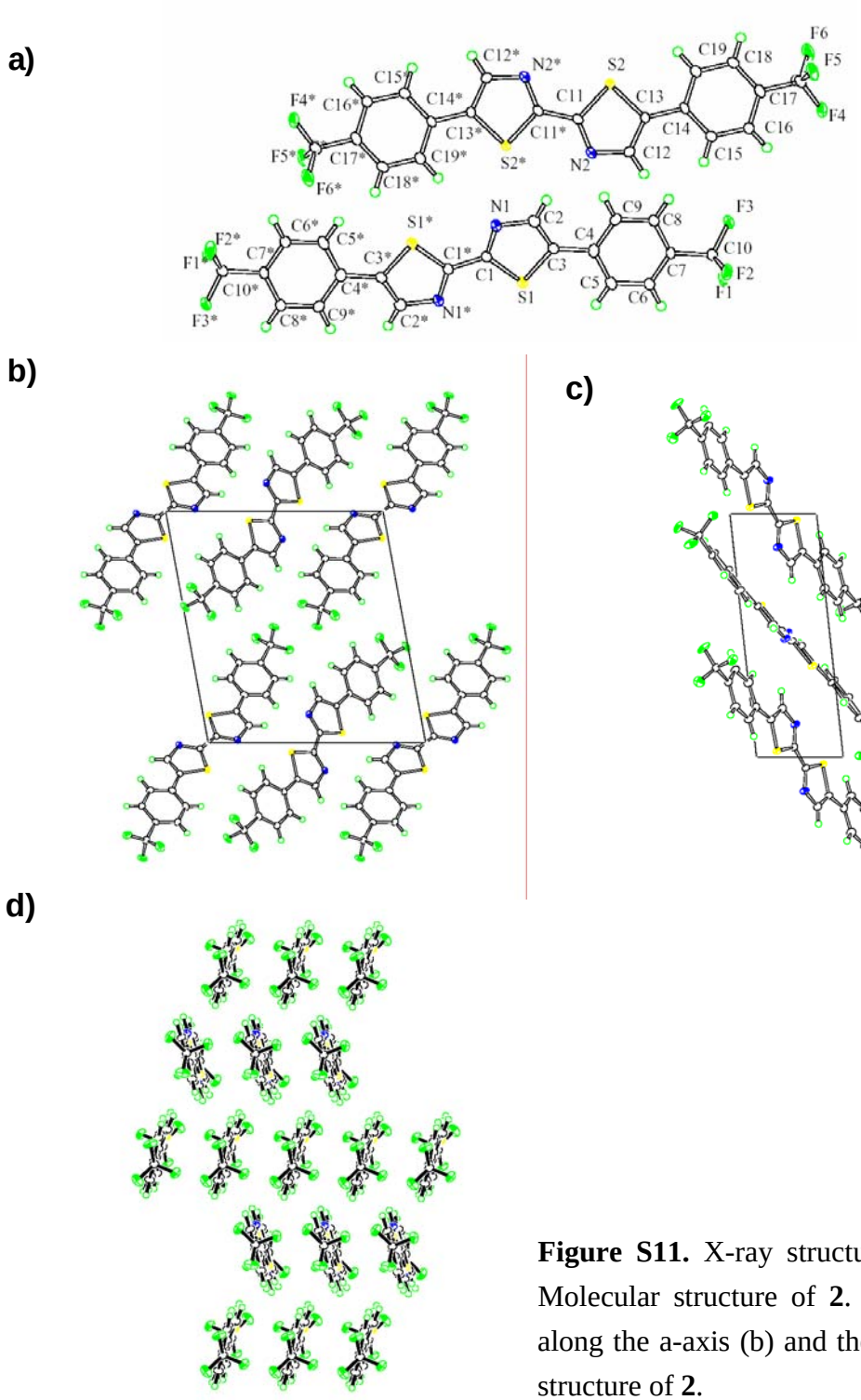

Figure S11. X-ray structure of compound **2**; (a) Molecular structure of **2**. Stacking structure of **2** along the a-axis (b) and the c-axis (c). (d) π–Stack structure of **2**.

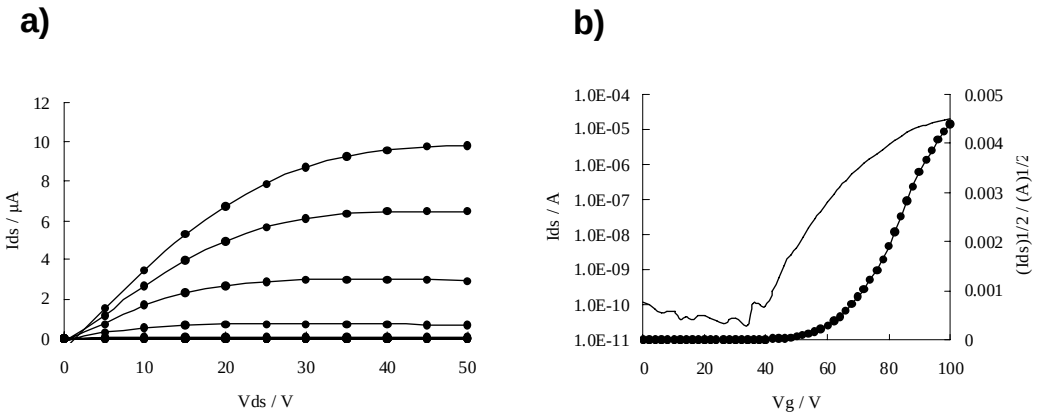

Figure S12. (a) Source-drain current (*I*ds) versus drain voltage (*V*ds) characteristics as a function of gate voltage (Vg) for OFET from compound **1** on SiO_2. (b) *I*ds and $Ids^{1/2}$ versus *V*g plots at *V*ds = +50 V.

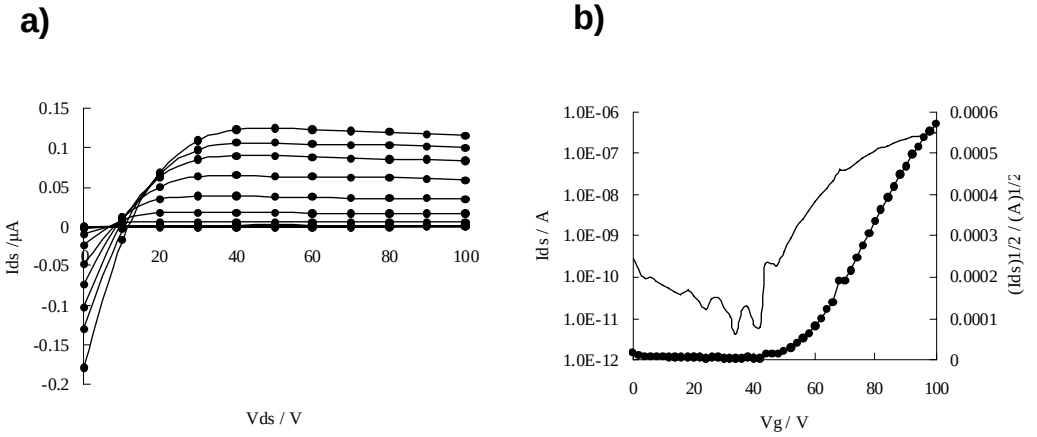

Figure S13. (a) Source-drain current (*I*ds) versus drain voltage (*V*ds) characteristics as a function of gate voltage (Vg) for OFET from compound **3** on SiO_2. (b) *I*ds and $Ids^{1/2}$ versus *V*g plots at *V*ds = +50 V.

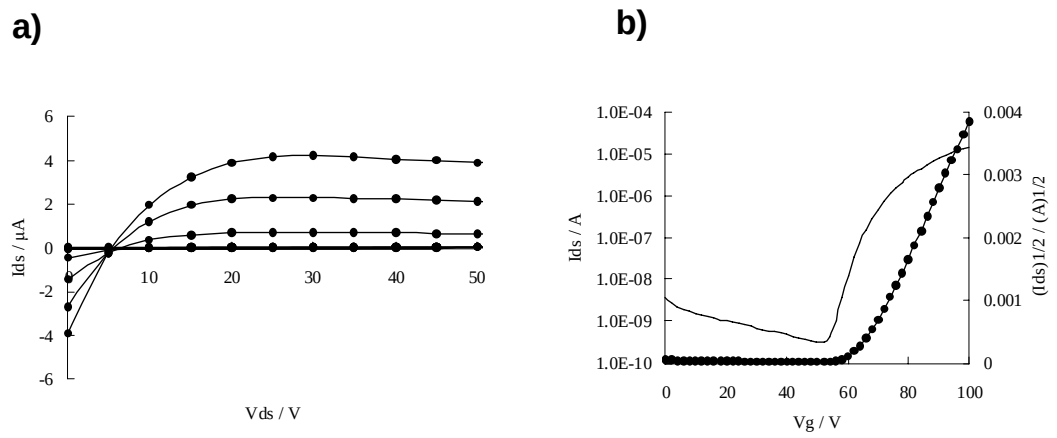

Figure S14. (a) Source-drain current (*I*ds) versus drain voltage (*V*ds) characteristics as a function of gate voltage (Vg) for OFET from compound **4** on SiO_2. (b) *I*ds and $Ids^{1/2}$ versus *V*g plots at *V*ds = +50 V.

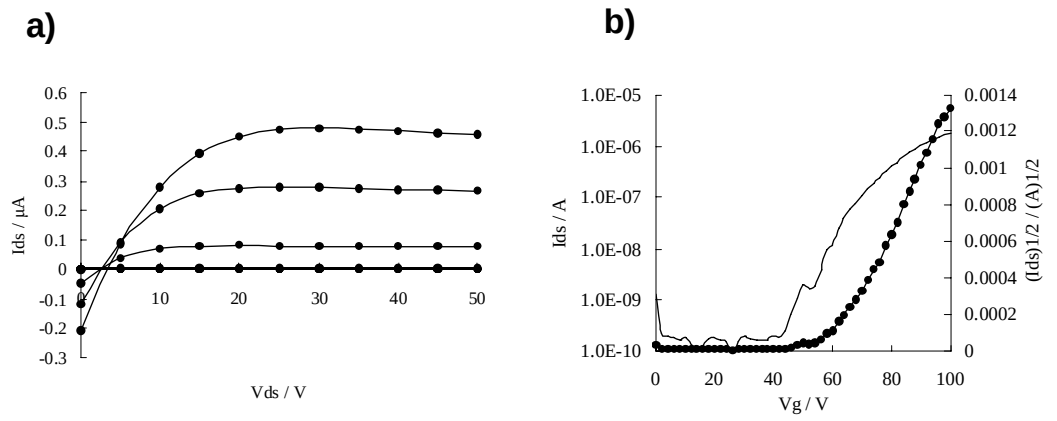

Figure S15. (a) Source-drain current (*I*ds) versus drain voltage (*V*ds) characteristics as a function of gate voltage (Vg) for OFET from compound **5** on SiO_2. (b) *I*ds and $Ids^{1/2}$ versus *V*g plots at *V*ds = +50 V.

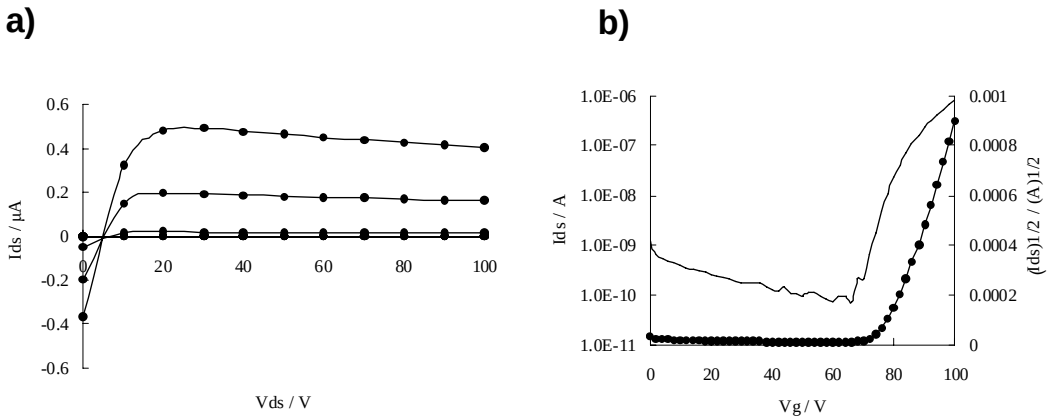

Figure S16. (a) Source-drain current (*I*ds) versus drain voltage (*V*ds) characteristics as a function of gate voltage (Vg) for OFET from compound **6** on SiO_2. (b) *I*ds and $Ids^{1/2}$ versus *V*g plots at *V*ds = +50 V.

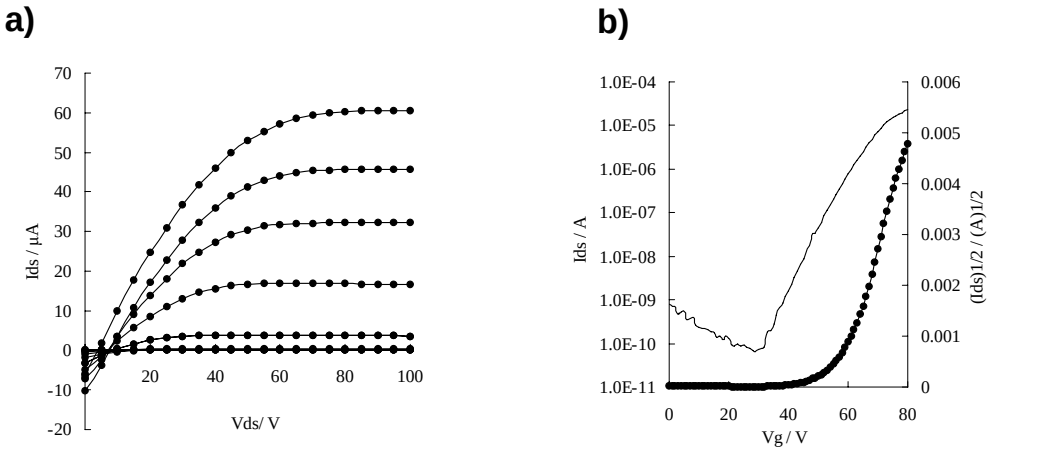

Figure S17. (a) Source-drain current (*I*ds) versus drain voltage (*V*ds) characteristics as a function of gate voltage (Vg) for OFET from compound **1** on HMDS treated SiO_2. (b) *I*ds and $Ids^{1/2}$ versus *V*g plots at *V*ds = +50 V.

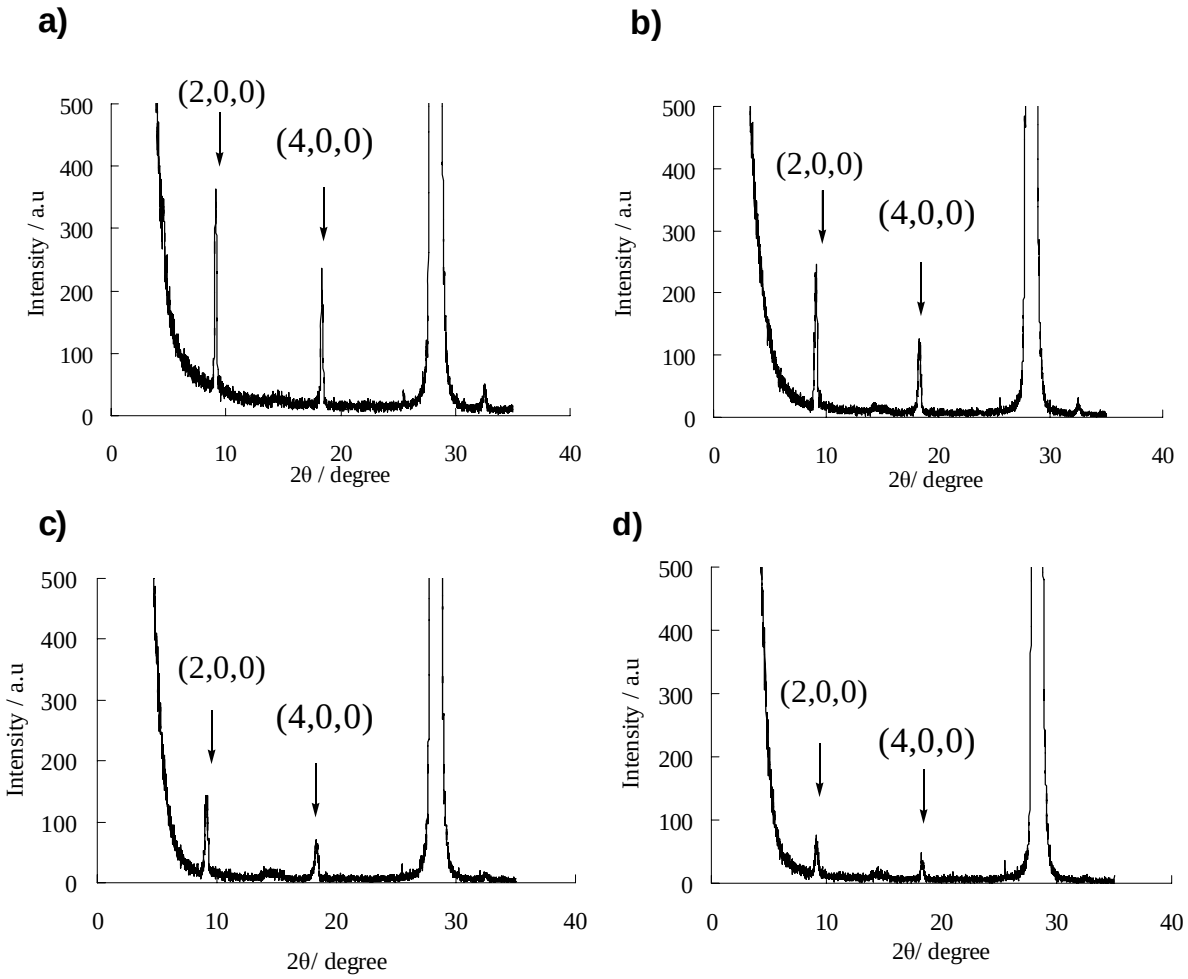

Figure S18. X-ray diffractograms from 50 nm films of **1** deposited on (a) SiO_2, (b) OTS-treated SiO_2 (c) HMDS-treated SiO_2 at room temperature and (d) SiO_2 at 50 ºC. Peaks are assigned from the powder pattern calculated from the single crystal structures using the program Mercury version 1.3.

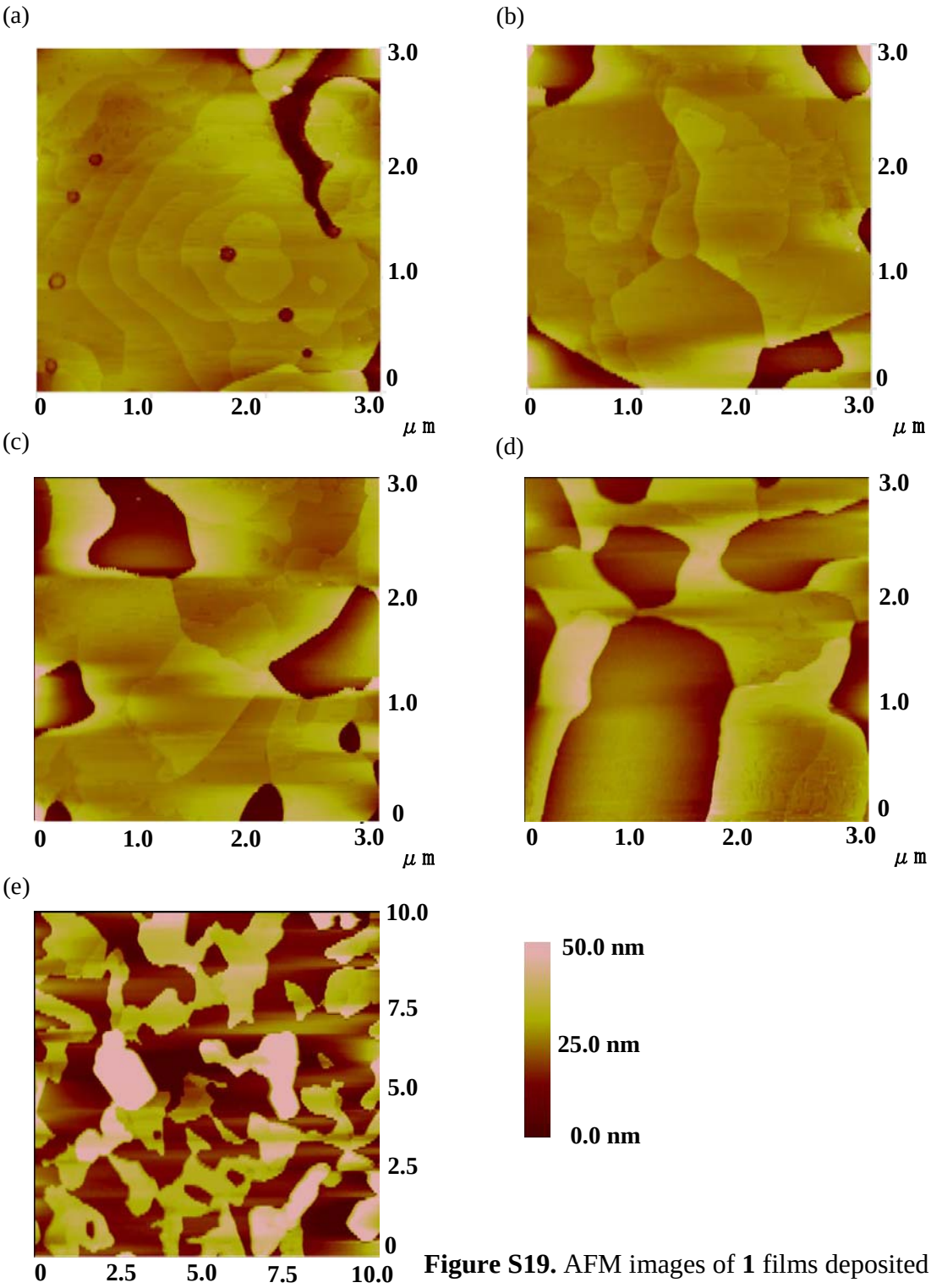

Figure S19. AFM images of **1** films deposited on (a) OTS at 25 ºC; (b) HMDS at 25 ºC; (c) SiO_2 at 25 ºC; (d),(e) SiO_2 at 50 ºC.

a)

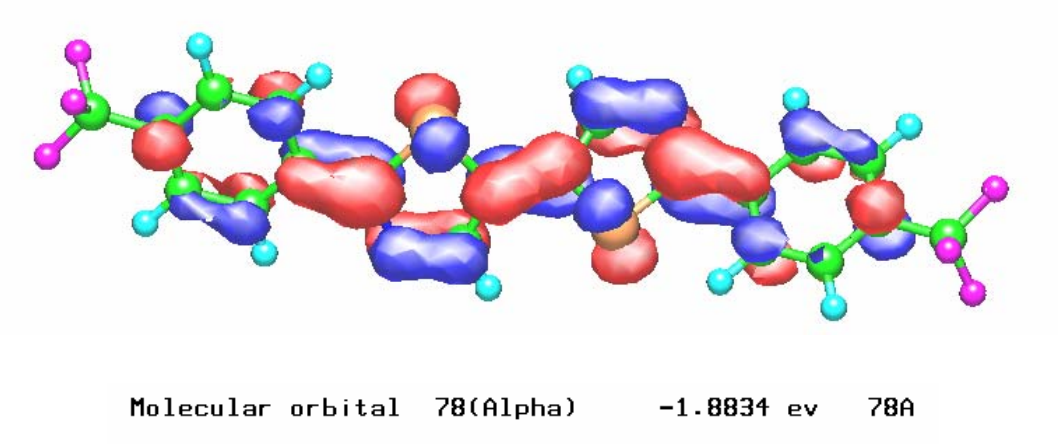

b)

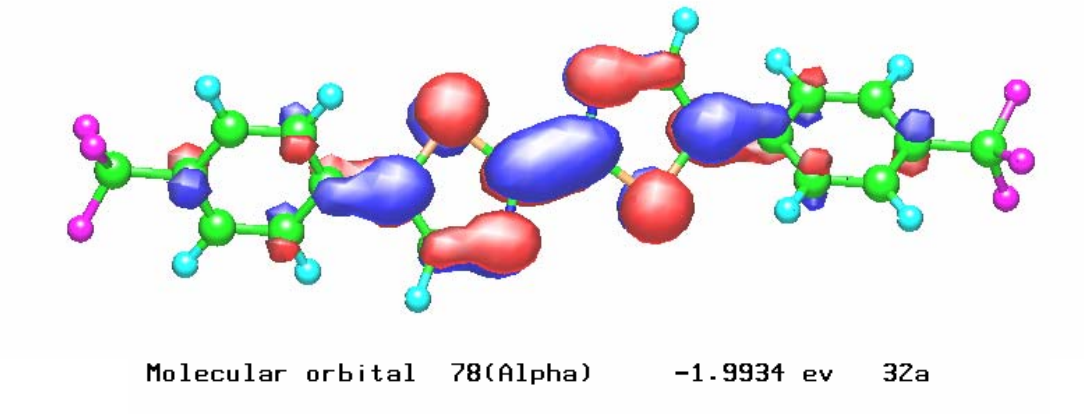

Figure S20.

LUMO of **1** (a) and **2** (b) calculated by the PM5 method.